Published in final edited form as:
J Phys Chem C Nanomater Interfaces. 2013 August 29; 117(34): 17367–17375. doi:10.1021/jp4010554.

Pump-Flow-Probe X-Ray Absorption Spectroscopy as a Tool for Studying Intermediate States of Photocatalytic Systems

Grigory Smolentsev[#,†,*], **Alexander Guda**[‡], **Xiaoyi Zhang**[&], **Kristoffer Haldrup**[§], **Eugen Andreiadis**[Δ], **Murielle Chavarot-Kerlidou**[Δ], **Sophie E. Canton**[#], **Maarten Nachtegaal**[†], **Vincent Artero**[Δ], and **Villy Sundstrom**[#]

[#]Lund University, Lund, 22100, Sweden [†]Paul Scherrer Insitute, Villigen, 5232, Switzerland [‡]Research center for nanoscale structure of matter, Southern Federal University, Rostov-on-Don, 344090, Russia [&]X-ray Science Division, Argonne National Laboratory, Argonne, IL, 60439, USA [§]Department of Physics, Danish Technical University, Copenhagen, Denmark [Δ]Laboratory of Chemistry and Biology of Metals, CEA,CNRS, University Joseph Fourier, Grenoble, France

Abstract

A new setup for pump-flow-probe X-ray absorption spectroscopy has been implemented at the SuperXAS beamline of the Swiss Light Source. It allows recording X-ray absorption spectra with a time resolution of tens of microseconds and high detection efficiency for samples with sub-mM concentrations. A continuous wave laser is used for the photoexcitation, with the distance between laser and X-ray beams and velocity of liquid flow determining the time delay, while the focusing of both beams and the flow speed define the time resolution. This method is compared with the alternative measurement technique that utilizes a 1 kHz repetition rate laser and multiple X-ray probe pulses. Such an experiment was performed at beamline 11ID-D of the Advanced Photon Source. Advantages, limitations and potential for improvement of the pump-flow-probe setup are discussed by analyzing the photon statistics. Both methods, with Co K-edge probing were applied to the investigation of a cobaloxime-based photo-catalytic reaction. The interplay between optimizing for efficient photoexcitation and time resolution as well as the effect of sample degradation for these two setups are discussed.

Keywords

XTA; Time-resolved spectroscopy; cobaloxime; XANES; Photocatalysis; cobaloxime; XANES; pump-probe; LITR XAS

Introduction

X-ray absorption spectroscopy (XAS) has a significant potential to allow clarification of the mechanisms of reactions catalyzed by metal complexes. Thanks to its element selectivity and sensitivity to electronic structure, XAS is well suited for probing the local atomic structure around the absorbing atom and the chemical state (oxidation and often spin states) of the catalytic center and can thus allow direct determination of the solution-state structure of reaction intermediates along a given catalytic cycle. For 3d elements the pre-edge region of K-edge XAS spectra and L-edge XAS are sensitive to the electronic configuration of the absorbing atom[1,2,3]; the position of the K-edge is mainly sensitive to the oxidation state (but

[*]**Corresponding Author**: grigory.smolentsev@psi.chtel: +41 56 310 51 73.

Europe PMC Funders Author Manuscripts

also depends on the coordination environment), while the X-ray absorption near edge (XANES) region of the K-edge spectra contains structural information arising from multiple scattering of photoelectrons.

Light-driven catalytic reactions such as water splitting[4,5,6,7,8,9], CO_2 activation[10] and selective oxidations[11,12] are of special interest for the development of environmentally benign catalytic processes[13] and production of solar fuels. Investigating the mechanisms of homogeneous multicomponent photocatalytic systems, time-resolved spectroscopic techniques with time-resolution in the microsecond range are often required. A typical photocatalytic multicomponent system has been described by Gray and coworkers[14] (see Fig. 1). The photosensitizer $[Ru(bpy)_3]^{2+}$ (bpy = 2,2′-bipyridine) is excited with light and its excited state is quenched by an electron relay compound methyl-viologen (MV^{2+}) [15,16]. The reduced viologen species ($MV^{\bullet+}$) then delivers an electron to a catalytic center, here cobaloxime. In order to evolve molecular hydrogen (H_2), sources of protons and electrons (sacrificial electron donor) are required. The Ru-sensitizer has to be re-reduced by a sacrificial electron donor facilitating absorption of one more photon and delivery of the second electron to the catalyst. In the absence of protons and an electrons source, hydrogen evolution is not possible and there will be a slow recovery to the initial state by back electron transfer. Since all main components are in solution and do not have specific interactions with each other, charge transfer and all subsequent reaction steps occur on diffusion-limited time scales. Therefore, the relevant intermediate states of the catalytic compound(s) often have lifetimes in the microsecond to ms range, depending on reactivity and concentrations.

Time-resolved X-ray absorption spectroscopy with picosecond time resolution is currently well developed. Pump-probe setups with kHz repetition rate exist[17,18,19,20,21,22,23]. They use synchrotron sources (that have X-ray pulses with MHz repetition rates) for probing and kHz lasers for sample excitation. Powerful optical laser pulses allow efficient excitation of the studied molecules (reported values are between 7 and 50 % for kHz pump-probe XAS). Achieving a large fraction of excited molecules in the probed volume has been one main requirement for the feasibility of such experiments, since only a small fraction (~10^{-3}) of the X-ray flux is used for probing due to the mismatch in laser vs X-ray pulse repetition rates. Only one X-ray pulse out of a thousand in the MHz pulse train delivered by the synchrotron ring might detect laser-induced changes in the sample that occur with kHz frequency. Another factor that affects the feasibility of such an experiment is the difference in optical and X-ray absorption cross sections. In order to improve the detection efficiency, setups with high laser pulse repetition rate (~1 MHz) have been developed recently[24,25]. At such high frequencies the filling pattern of the storage ring becomes important and the much larger bunch separation at large storage rings allows to obtain higher efficiency for the given laser repetition rate. Since it is extremely difficult to refresh the sample with such high repetition rate, the application of this pump-probe scheme is currently limited to compounds with short-lived intermediates (<1 microsecond) to avoid complications arising from the build-up of long-lived transients. On the other hand, long-lived transients with a lifetime in the microsecond range can be very efficiently measured with kHz laser excitation and using X-ray probe pulses that follow with MHz frequency as described in the experimental method section below. For similar applications the use of a laser with a repetition rate of 10-200 kHz allows to get maximal efficiency and such setups are under development at the SuperXAS beamline of SLS and at a few beamlines of the APS.

There are several challenges related to the application of time-resolved XAS to study the structure of intermediate states of multicomponent photocatalysts. First, the (relative) amounts of intermediates formed are usually low, and even if the chromophore is efficiently excited by the laser, the diffusion-limited character of the electron transfer reduces the

percentage of intermediates in a given time window. Second, under realistic operating conditions, the concentration of the photocatalyst is usually low (~0.1 mM). A significant increase of this concentration can lead to undesired effects, such as aggregation of complexes and formation of bimetallic species[26].

Examples of X-ray absorption experiments with microsecond time resolution are rare in the scientific literature. After a few pioneering works [27,28,29,30], this field appears to have been almost abandoned. In ref.[27] the combination of rapid-flow and excitation with a CW laser was used and a time resolution of ~1μs was achieved.

In this article we present the first application of time-resolved X-ray absorption spectroscopy with microsecond time resolution to a multicomponent photocatalytic system. A pump-flow-probe setup with CW laser excitation having high detection efficiency and thus the ability to measure time-resolved spectra at sub-mM concentrations has been developed and applied to the cobaloxime-based photocatalytic system. The results obtained with this pump-flow-probe XAS setup are compared with those obtained using a time-resolved measurement technique that utilizes a pump-sequential-probes scheme with kHz pulsed picosecond sample excitation.

Experimental method

Samples

The catalyst $[Co(dpgBF_2)_2(OH_2)_2]$ ($dpgH_2$ = diphenylglyoxime) was prepared as previously described[31] and is shown in Figure 1. $[Ru(bpy)_3]Cl_2$, methyl viologen dichloride ($MVCl_2$), NH_4PF_6 and NBu_4PF_6 were purchased from Sigma-Aldrich and used without further purification. As photo-sensitizer and electron-relay, $[Ru(bpy)_3](PF_6)_2$ and $MV(PF_6)_2$ were prepared from NH_4PF_6 and $[Ru(bpy)_3]Cl_2$ or $MVCl_2$ respectively, following a standard anion-exchange procedure. The solid-state metal complexes were handled in air. Anhydrous acetonitrile was purchased from Fisher Scientific.

For the pump-flow-probe experiments the sample consisted of an acetonitrile solution of $[Ru(bpy)_3](PF_6)_2$ (0.4 mM), $MV(PF_6)_2$ (8 mM), tetrabutylammonium hexafluorophosphate NBu_4PF_6 (0.1M) and $[Co(dpgBF_2)_2(OH_2)_2]$ (0.3-0.7 mM). The same sample composition was used for the pump-sequential-probes experiment but with significantly higher concentrations: $[Ru(bpy)_3](PF_6)_2$ 3 mM, $MV(PF_6)_2$ 8 mM, NBu_4PF_6 0.1 M and $[Co(dpgBF_2)_2(OH_2)_2]$ 1-2 mM. The optical density of the samples was 0.5 for pump-flow-probe conditions (at the 447-nm excitation wavelength with 1 mm sample thickness), and 0.2 for pump-sequential-probes conditions (525 nm excitation and also 0.6 mm sample thickness). The Co-compound used for the measurements reported in this study was not very soluble in CH_3CN and the solution had to be filtered before use, leading to an uncertainty in final sample concentrations stated above. After the time resolved XAS measurements, the identity of the unused sample was checked with cyclic voltammetry and electron spray ionization mass spectroscopy and the presence of $[Co(dpg)_3(BF)_2]^+$ was detected[32]. This contamination does not significantly influence the main aim of this work, which is to compare and evaluate the two different excitation and detection schemes for microsecond time resolved XAS. However, the presence of this species in the reaction mixture may contribute to the measured XAS spectra and kinetics, and we will therefore refrain from a detailed analysis of the transient XAS spectra. Such an analysis aiming at more detailed mechanistic information has to await further optimization of the conditions of the pump-flow-probe experiment. For both setups the freshly prepared sample solution was degassed with N_2 at least 30 minutes before the experiment and continuously purged and kept under N_2 during the experiment.

Pump-flow-probe experiment

The conceptual idea of this experimental setup is to perform time-resolved measurements by focusing on a fast flowing jet a continuous wave (CW) laser beam for sample excitation, spatially separated at a variable distance from an X-ray probe beam. Figure 2 shows in schematic form the experimental setup, with the sample circulating in the flow system through a capillary where the interaction with the pump and probe beams take place. The CW laser, is focused on the capillary (1 mm diameter, 10 μm wall thickness), and excites the sample and downstream the X-ray beam probes it. The distance between the two beams **d** and the flow speed **v** of the liquid together determine the time delay, while the focusing of the laser and the X-ray beams and the velocity profile of the sample solution define the effective time resolution. Therefore, we refer to this experiment as *pump-flow-probe*.

In order to achieve efficient excitation of $[Ru(bpy)_3]^{2+}$, we selected a laser with a 447 nm wavelength and 1 W power (CNI lasers MDL-III-447). The laser beam was focused with cylindrical lenses to a spot size of 0.1*1 mm^2 (vertical*horizontal) at the sample position and the X-ray beam was focused to a 0.1*0.1 mm^2 spot. The use of a capillary and closed flow system allowed the sample to be kept under oxygen-free conditions. For the experiments presented here, the average flow speed in the probed region in the capillary was 3 m/s corresponding to a 333 μs delay between pump and probe per millimeter of spatial separation between laser and X-ray beams. XAS measurements were performed in differential mode where the X-ray energy is first changed, then the XAS signal is measured with laser on for 1-30 s, following which the XAS signal without laser is measured for the same time. The X-ray energy is then stepped to the next energy-point and the same measurement sequence is repeated.

In order to control the spatial separation between laser and X-ray beams one has to first determine the position where they overlap. A tungsten pin-hole with 100 μm diameter and 50 μm thickness was used to find the X-ray beam position, and then to achieve spatial overlap of the beams the transmitted laser intensity through the pinhole was maximized by adjusting the alignment mirror (3). As an alternative, optical fluorescence induced by both the pump and probe beams was found to be sufficiently intense to allow accurate control of beam positions by webcam-imaging of the sample. A neutral density filter with an optical density of ~7 was used during the alignment in order to reduce the fluorescence induced by the laser and registered by the camera.

The pump-flow-probe measurements were performed at the SuperXAS beamline of the Swiss Light Source (SLS). The storage ring was operated in the top-up mode (400 mA). XAS spectra were detected in the fluorescence mode (Co Kα line) using an energy-resolving 13-element germanium detector (Canberra) with an additional Z-1 (Fe) filter. A double-crystal Si[111] monochromator was used to define and scan the X-ray energy, while a Rh-coated toroidal mirror provided 0.1*0.1 mm^2 focussing of the X-ray beam on the sample position.

Pump-sequential-probes experiment

Pump-sequential-probes measurements were performed at the 11ID-D beamline of the Advanced Photon Source (APS) using a highly optimized setup for Time-Resolved XAS which has been described in detail elsewhere [18]. In contrast to experiments aiming at picosecond time resolution and thus using only one X-ray bunch from the storage ring to probe the exited state after each laser pulse, the present experiment utilized a train of X-ray pulses with a separation of 153 ns from the APS storage ring operating in 24-bunch mode to record a series of spectra. Thus, the time evolution of the transient XAS signal was probed at successive time delays of n*153 ns after the excitation event. Therefore, we refer to this type

of experiment as *pump-sequential-probes*. The pump pulses were provided by the Nd:YLF regenerative amplifier laser installed at the beamline, and the second harmonic at 527 nm (pulse energy of 0.6 mJ at 1 kHz repetition rate, ~5 ps (fwhm) pulse duration and 0.8 - 1 mm spot size) was used in the present experiments. The shortest time delay between laser and X-ray pulses investigated here was 100 ps. The X-ray beam had ~10^6 photons/pulse, focused to a spot smaller than the sample jet diameter, and XAS data sets were acquired in fluorescence mode using the dedicated pulse-to-pulse digitization setup of the beamline. The sample jet diameter was 0.6 mm.

Results and discussion

Excitation conditions and time resolution - Simulations

Based on the reaction scheme and the rate equations given in the SI we performed simulations of the time evolution of intermediate concentrations to guide the choice of experimental conditions towards maximizing the expected transient signal. In the pump-flow-probe experiment the sample (or, more precisely, each elementary volume flowing through the capillary) is excited by the CW laser during the time window that is defined by the flow speed and laser spot size. The typical excitation time is on the order of 20 μs which is quite different from the conditions of pump-probe experiments with pulsed lasers that usually have pulse durations <100 ps. The excitation time of 20 μs corresponds to 100 μm focusing of the laser beam and flow speed of 5 m/s, it can be used as lower limit for the excitation time that gives also lower estimate for the concentration of reaction intermediates. The irradiated volume (1 mm×0.1 mm spot size and 1 mm thickness) receives 4.4×10^{13} photons from the 1-W laser at 447 nm during 20 μs. The number of chromophores (0.4 mM concentration) in this volume is 1.9×10^{13}. In the case of pulsed 1 kHz excitation from the 527 nm laser with 0.6 W average power, there are 1.5×10^{15} photons per pulse, which is comparable with the 0.8×10^{15} chromophores (3 mM concentration) in the irradiated volume (1 mm×1 mm spot size and 0.6 mm thickness).

In the SI we compare CW and pulsed excitation schemes in detail by simulating the concentration dynamics following photo-excitation of the multicomponent photocatalytic system consisting of $[Ru(bpy)_3]^{2+}$ as the photosensitizer/chromophore, the cobaloxime $[Co^{II}(dpgBF_2)_2(OH_2)_2]$ as the final electron acceptor and MV^{2+} as the electron relay. The main results of these simulations are the following:

- CW laser excitation allows the accumulation of more than 10 % of $[Ru(bpy)_3]^{3+}$, formed mainly as a result of quenching of $[Ru(bpy)_3]^{2+*}$ by MV^{2+}. There is a saturation level of the $[Ru(bpy)_3]^{3+}$ concentration that mainly depends on the laser power (increase of illumination time will not lead to the increase of $[Ru(bpy)_3]^{3+}$ concentration beyond this level).
- Using the 1-W CW laser it is possible to obtain a few percents of the Co catalyst compound in its intermediate state(s). This fraction is comparable with what can be achieved with efficient pulsed laser excitation.
- With relatively low concentrations of the Ru chromophore (~0.4 mM, which corresponds to the optimal optical density for a 1 mm sample excited with a 447 nm laser) and Co catalyst (~0.3 mM), the intermediate states of Co appear in the tens of microseconds time range.

In the pump-sequential-probe approach, the flow speed defines how long the probe volume overlaps with the excited volume and therefore determines the longest time delays accessible by this method. A typically used liquid jet flow speed for such experiments with picosecond-nanosecond time resolution is ~2 m/s, which implies that after ~25 μs half of the

excited volume has left the probe region in the jet (assuming 0.1 mm focusing for both laser and X-ray beams). This effect will therefore give the main contribution to the decay of the transient signal in the >10 μs time range. In the case of large laser spot (~1 mm) and a small X-ray spot (~0.1 mm) the accessible time range can be several times longer. In the pump-flow-probe method the flow speed and flow profile as well as the laser spot size define not only the time resolution but also the number of absorbed photons, and therefore the fraction of excited chromophores. This is discussed in detail in the SI.

When a capillary is used to maintain anaerobic conditions one has to take into account that the flow speed in the capillary is not constant across its diameter. Under laminar flow conditions it changes from 0 near the walls to twice the average velocity ($v_{average}$) in the center. This implies that at a beam separation distance, *d*, corresponding to a particular delay time between laser excitation and X-ray probing, also events corresponding to longer delay times contribute to the measured XAS signal. This effect is described quantitatively in the SI and one can notice the tail of the probability distribution function at longer times (see figure S1 in the SI). The time resolution of the pump-flow-probe experiment can be characterized by the full width at half maximum, Γ, of the distribution function shown in Fig. S1 and its standard deviation, σ. Under conditions corresponding to the transient XAS spectra shown below the expected time resolution is Γ = 32 μs and σ = 40 μs. The corresponding values of these parameters for the model with constant flow speed, but with the same average velocity are Γ = 47 μs and σ = 20 μs. It is relevant to note that for capillary flow the time resolution thus depends not only on the size of the beams and flow speed, but also on the spatial separation between beams. Therefore, achieving very good time resolution in measurements with very long delay times is difficult with a capillary for the sample flow; a free flowing jet should eliminate this problem.

Requirements for detectors

Measurements of XAS of dilute samples in fluorescence mode, as in the experiments discussed here, requires efficient separation of elastically scattered and fluorescent X-ray photons. This can be achieved using energy-resolving solid state detectors or with dispersive optics (crystals)[33,34,35,36]. The use of dispersive optics usually allows to reach superior energy resolution, but at the expense of solid angle and thus signal intensity. Time-resolved experiments with dispersive optics recently attracted some interest and it has been shown that even time-resolved RIXS spectroscopy (a combination of XAS and X-ray emission) is possible[37]. For the pump-flow-probe experiment reported here we used an energy-resolving multi-element germanium detector, which has a sufficient energy resolution to resolve the elastic and fluorescent peaks, and which could be placed relatively close to the sample to achieve a reasonably high count rate.

The requirements on detectors in the pump-sequential-probes scheme are completely different. They have to be fast enough to separate X-ray bunches that arrive with a frequency of a few MHz. Alternatively, X-ray choppers can be used in combination with a slow detector, but such technology is more popular for scattering experiments[38,39,40,41](even if electronic gating of modern 2D detectors is also possible[42,43]). To the best of our knowledge there are no currently available detectors that are simultaneously fast and have good energy resolution. At an early stage of development, multielement Ge detectors were used for pump-probe experiments at the APS[44]11-ID-D end-station, but after the beamline upgrade, and with the extensive use of the 24-bunch mode at the APS, this detector was found to be too slow and easily overloaded. Avalanche photodiodes (APD) or photomultiplier tubes (PMT) allow to separate X-ray pulses that follow with a period of 100 ns or more, but does not provide energy resolution. The current setup at this instrument uses

a combination of Z—1 filters (Fe in our case) and Soller slits[45,46] with conical geometry to reduce the background from elastically scattered X-ray photons.

Comparison of experimental results

The kinetic data that are obtained from pump-sequential-probes measurements are additional information to that obtained from the pump-flow-probe experiment. A series of time points is measured in a single pump-sequential-probes experiment, while using the pump-flow-probe method only one time point is collected at each setting of the laser and X-ray beam separation distance.

In Fig. 3, transient XAS spectra corresponding to a sequence of different probe pulses following the laser pulse are shown for the pump-sequential-probes method. No discernible difference signal is evident for the bunch that corresponds to the 100 ps delay, while at 306 ns delay a difference signal is clearly evident. The absence of a signal at 100 ps is expected from the kinetic simulations and it further indicates that there is no direct laser excitation of the Co center at 527 nm and that there is no specific interaction between the components (formation of aggregates or supramolecular complexes) that can lead to fast electron transfer. Each individual transient spectrum is quite noisy, but there is high temporal oversampling over the lifetime of the species. As a first approximation one can average a series of spectra corresponding to a rather wide time window, but shorter than the lifetime of the transient species. There are data analysis methods that allows to extract the structure of intermediates from time-resolved XAFS data sets without binning of the spectra and therefore without loosing the time resolution [47]. In many cases structural parameters correlate with the percentage of intermediate and both these parameters cannot be determined simultaneously. Therefore it is important to have good estimate of the percentage of the intermediate from independent experiments in order to obtain the high accuracy of structure determination.

The pump-flow-probe experiment allows information about the reaction kinetics to be obtained by varying the spatial separation between the laser and the X-ray beams, while keeping the X-ray energy fixed at the spectral feature of particular interest, e.g. at the position where the difference signal exhibits the largest magnitude. Figure 4 shows the data from such a measurement series, and from the discussion above and in the SI (section: time resolution) we conclude that there is significant contribution of the temporal response function to the rise time of the signal shown in Fig. 4. Note that if the reaction kinetics in the considered time-range are simple, for example, if there is only one intermediate state present, then the extraction of the structure of the intermediate is possible by using either a single spectrum or a longer series of averaged spectra. In this case the two time-resolved XAS methods can be considered equivalent.

In the pump-sequential-probes experiment no significant temporal evolution of the difference spectrum was observed in the range 150 ns-3.7 μs, justifying the averaging of the time series to improve S/N. Pump-flow-probe measurements were performed for 100 μs delay between pump and probe. For both the pump-sequential-probes and pump-flow-probe experiments we have calculated the averaged spectrum and the error bars analyzing the series of spectra using standard statistical methods. Figure 5 shows that both methods produce similar difference spectra; a small difference of the width of the first peak is however discernible and could be due to the mixing of intermediates with different concentration ratios in these two spectra. The shape of the spectra is typical for Co reduction (see for example ref [48] and figures S4 and S5 in the SI). The first peak corresponds to the shift of the edge position to lower energy due to the oxidation state change of Co and partially due to the structural changes in the molecule. From a comparison of the average amplitude of the signal of the pump-flow-probe experiment with previously published data

Europe PMC Funders Author Manuscripts

for a RuCo supramolecular complex[48] one can note that the transient signal is more than 10 times lower than in the case of the RuCo supramolecular complex and therefore high detection efficiency is essential. The amplitude of the signal measured using the pump-sequential-probes method is more than twice that measured using the pump-flow-probe method (from the estimates summarized in the SI we expected a stronger signal from the pump-flow-probe method). This indicates that possibly the assumption of 30% photo-excitation was too conservative and in reality it is much higher. Alternatively, it could be that at our experimental conditions and for our sample the lifetime of intermediate is much shorter than previously reported[14] and therefore we detected a lower percentage of intermediate due to a partial decay during ~100 μs.

In Table 1 we summarize relevant experimental parameters for both experiments, including both expected and observed counting statistics for the X-ray photons. In SI we briefly discuss and compare these parameters of the two different methods. The relatively high noise of individual spectra measured with the pump-sequential-probes method is due to a mismatch of the repetition rates of the laser pump and X-ray probe pulses. However, since the full series of time points are collected during the same energy scan, binning of many spectra (as shown in Fig. 5) allows the construction of spectra with better signal-to-noise ratio. The use of a Soller slit in combination with a Z-1 filter for the pump-sequential-probes method allowed to suppress a significant fraction of the elastic scattering, and even if the APD detectors do not have energy resolution, this detection scheme is quite efficient for samples with concentrations of the studied compound down to 1 mM. The main limitation of the pump-flow-probe experiment in the current setup is the use of a multi-element Ge-detector, which accepts maximum ~$5*10^4$ counts/s per channel, a significant fraction of which are elastically scattered photons. In order to avoid saturation, the detector had to be placed far from the sample decreasing the solid angle of detection. With energy resolving detectors, there is significant potential for using the pump-flow-probe method for measurements of weak signals from dilute samples due to the possibility of discriminating the elastic and fluorescent photons.

Sample degradation

As a final point in this comparative study we consider sample degradation, a particular problem that often appears during time-resolved X-ray absorption measurements due to the often-times long exposures to both X-ray and laser beams. Almost all setups that are currently developed for picosecond experiments use relatively large sample volumes (at least 30 ml) circulating in a flow system to minimize the effect of sample damage on the spectra. The cause of sample degradation varies significantly between compounds. Sometimes it is related to the highly increased reactivity of the optically excited species compared to the ground state[49]; in other cases the X-ray beam directly reduces the sample. Figure 6 shows noticeable spectral changes due to reduction of the sample after 8 hours of measurements with the pump-sequential-probes setup (lower graphs), while the spectra are essentially unchanged in the case of pump-flow-probe measurements (upper graphs). Data were accumulated for a longer time (up to 18 hours) using the pump-sequential-probes method where the degradation effect was even more dramatic (Fig. 6, red trace), while for the pump-flow-probe experiment the statistics was sufficient after 8 hours and accordingly we did not have data sets for longer irradiation times. One of the reasons behind this difference in radiation damage is the much higher photon flux on the sample at the undulator beamline of the APS in comparison to the bending-magnet source used at SLS. Another contribution may come from the excitation of the sample with powerful laser pulses in the pump-sequential-probes experiment, while the CW laser used in the pump-flow-probe experiment provides a comparatively much gentler excitation in terms of peak laser flux.

As summarized in Table 1, the total dose of X-ray photons required to accumulate the spectra shown in Fig 5 is 4 times higher for the pump-sequential-probes method, but the dose of laser photons is 3 times lower. In order to avoid spectral contribution from the radiation damaged sample we used only the first 40 scans for the pump-sequential-probes spectrum shown in figures 3 and 5, which corresponds to approximately the first 3 hours of accumulation. As one can see from Fig. 6 radiation damage has the character of Co reduction (shift of the absorption edge to lower energies). Laser-initiated reduction of the sample that is reduced already due to the radiation damage is not very probable. We therefore expect that the radiation damaged part of the sample does not contribute to the measured transient signal, although the kinetics may of course be affected by the lower effective concentration of the catalytic compound. This means that the radiation damage will lead only to an overall decrease of the amplitude of the transient signal in agreement with the experimentally observed trends (see Fig. S7 in the SI).

In order to identify the origin of the sample damage and establish “safe” experimental conditions where the measured transient spectra are not affected, we have compared in the SI (Fig S6) how different experimental conditions influence the X-ray absorption spectra. By comparing spectra that were measured with either the same laser dose but very different X-ray dose, or the same X-ray dose but very different laser dose it is seen that the X-ray beam mainly contributes to the sample damage, while the laser dose only contributes weakly in these experiments. Less sample degradation observed during the pump-flow-probe experiment with lower incident X-ray flux is an argument to consider when analyzing the feasibility of different time-resolved X-ray absorption experiments.

Conclusion

The pump-flow-probe and pump-sequential-probes methods for time-resolved X-ray spectroscopy are complementary in terms of time resolution. In some cases for multicomponent photocatalytic systems the same structural information about the reaction intermediates can be obtained using both pump-sequential-probes and pump-flow-probe methods by a rational choice of sample concentrations with the aid of kinetic simulations. Advantages of the pump-flow-probe setup are its compactness and transferability, as the method does not rely on an ultrafast pulsed laser synchronized to the storage ring. Modern CW diode or diode-pumped solid state lasers are portable and can be easily moved between different synchrotron sources. Also, the method does not require any special data acquisition electronics and the experiment does not depend on details of the filling mode of the storage ring. For further development of the pump-flow-probe setup the use of a solid state detector with higher achievable count rates (possibly in combination with Soller slits) as well as the development of a dedicated environmental chamber for open jet experiments under anaerobic conditions are the most important directions. The main requirement for beamlines for the pump-flow-probe experiments is that they obtain at least a moderate X-ray focusing (~100 μm) in the vertical direction.

Supplementary Material

Refer to Web version on PubMed Central for supplementary material.

Acknowledgments

The authors would like to thank M. Willimann and J. Szlachetko for their help during the experiments. Use of the Advanced Photon Source was supported by the U.S. Department of Energy, Office of Science, Office of Basic Energy Sciences, under Contract No. DE-AC02-06CH11357. This work is supported by the European Research Council under the European Union’s Seventh Framework Programme (FP/2007-2013) with an ERC Advanced investigator grant to V. Sundström - VISCHEM 226136 and an ERC starting grant to V. Artero - photocatH2ode

306398. The COST Action CM1202 PERSPECT-H2O is also acknowledged. The Swiss Light Source is thanked for the provision of beam time. G.S. and M.N would like to thank the Swiss National Science Foundation for funding of research. S.E.C acknowledges funding from the Swedish Research Council and A.G. would like to thank Russian Ministry of Education for the financial support (project #11.519.11.3005). We thank three anonymous reviewers for their detailed and constructive comments that significantly improved the manuscript.

References

(1). Westre TE, Kennepohl P, DeWitt JG, Hedman B, Hodgson KO, Solomon EI. A Multiplet Analysis of Fe K-Edge 1s → 3d Pre-Edge Features of Iron Complexes. J. Am. Chem. Soc. 1997; 119:6297–6314.

(2). DeBeer George S, Petrenko T, Neese F. Prediction of Iron K-Edge Absorption Spectra Using Time-Dependent Density Functional Theory†. J. Phys. Chem. A. 2008; 112:12936–12943. [PubMed: 18698746]

(3). De Groot F. High-Resolution X-ray Emission and X-ray Absorption Spectroscopy. Chem. Rev. 2001; 101:1779–1808. [PubMed: 11709999]

(4). Inagaki A, Akita M. Visible-Light Promoted Bimetallic Catalysis. Coord. Chem. Rev. 2010; 254:1220–1239.

(5). Losse S, Vos JG, Rau S. Catalytic Hydrogen Production at Cobalt Centres. Coord. Chem. Rev. 2010; 254:2492–2504.

(6). Artero V, Fontecave M. Light-Driven Bioinspired Water Splitting: Recent Developments in Photoelectrode Materials. Comptes Rendus Chimie. 2011; 14:799–810.

(7). Tinker LL, McDaniel ND, Bernhard S. Progress Towards Solar-Powered Homogeneous Water Photolysis. J. Mater. Chem. 2009; 19:3328–3337.

(8). Artero V, Chavarot-Kerlidou M, Fontecave M. Splitting Water with Cobalt. Angew. Chem. Int. Ed. 2011; 50:7238–7266.

(9). Andreiadis ES, Chavarot-Kerlidou M, Fontecave M, Artero V. Artificial Photosynthesis: From Molecular Catalysts for Light-driven Water Splitting to Photoelectrochemical Cells. Photochem. Photobiol. 2011; 87:946–964. [PubMed: 21740444]

(10). Morris AJ, Meyer GJ, Fujita E. Molecular Approaches to the Photocatalytic Reduction of Carbon Dioxide for Solar Fuels. Acc. Chem. Res. 2009; 42:1983–1994. [PubMed: 19928829]

(11). Guillo P, Hamelin O, Batat P, Jonusauskas G, McClenaghan ND, Ménage S. Photocatalyzed Sulfide Oxygenation with Water as the Unique Oxygen Atom Source. Inorg. Chem. 2012; 51:2222–2230. [PubMed: 22296643]

(12). Hamelin O, Guillo P, Loiseau F, Boissonnet M-F, Ménage S. A Dyad as Photocatalyst for Light-Driven Sulfide Oxygenation with Water As the Unique Oxygen Atom Source. Inorg. Chem. 2011; 50:7952–7954. [PubMed: 21793512]

(13). Yoon TP, Ischay MA, Du J. Visible Light Photocatalysis as a Greener Approach to Photochemical Synthesis. Nature Chem. 2010; 2:527–532. [PubMed: 20571569]

(14). Dempsey JL, Winkler JR, Gray HB. Kinetics of Electron Transfer Reactions of H2-Evolving Cobalt Diglyoxime Catalysts. J. Am. Chem. Soc. 2010; 132:1060–1065. [PubMed: 20043639]

(15). Esswein AJ, Nocera DG. Hydrogen Production by Molecular Photocatalysis. Chem. Rev. 2007; 107:4022–4047. [PubMed: 17927155]

(16). Summers LA. Diquaternary Salts of 4,4′-Bipyridine as Electron Relays for the Photoreduction of Water. J. Heterocyclic Chem. 1991; 28:827–842.

(17). Chen LX, Jager WJ, Jennings G, Gosztola DJ, Munkholm A, Hessler JP. Capturing a Photoexcited Molecular Structure Through Time-Domain X-ray Absorption Fine Structure. Science. 2001; 292:262–264. [PubMed: 11303096]

(18). Chen LX, Zhang X, Lockard JV, Stickrath AB, Attenkofer K, Jennings G, Liu DJ. Excited-State Molecular Structures Captured by X-ray Transient Absorption Spectroscopy: a Decade and Beyond. Acta. Crystal. A. 2010; 66:240–251.

(19). Saes M, Bressler C, Abela R, Grolimund D, Johnson S, Heimann P, Chergui M. Observing Photochemical Transients by Ultrafast X-Ray Absorption Spectroscopy. Phys. Rev. Lett. 2003; 90:047403. [PubMed: 12570459]

(20). Saes M, van Mourik F, Gawelda W, Kaiser M, Chergui M, Bressler C, Grolimund D, Abela R, Glover TE, Heimann PA, et al. A Setup for Ultrafast Time-Resolved X-Ray Absorption Spectroscopy. Rev. Sci. Instrum. 2004; 75:24–30.

(21). Zhang X, Smolentsev G, Guo J, Attenkofer K, Kurtz C, Jennings G, Lockard JV, Stickrath AB, Chen LX. Visualizing Interfacial Charge Transfer in Ru-Dye-Sensitized TiO2 Nanoparticles Using X-ray Transient Absorption Spectroscopy. J. Phys. Chem. Lett. 2011; 2:628–632.

(22). Sato T, Nozawa S, Ichiyanagi K, Tomita A, Chollet M, Ichikawa H, Fujii H, Adachi S, Koshihara S. Capturing Molecular Structural Dynamics by 100 ps Time-Resolved X-ray Absorption Spectroscopy. J. Synchrotron Rad. 2008; 16:110–115.

(23). Bressler C, Chergui M. Molecular Structural Dynamics Probed by Ultrafast X-Ray Absorption Spectroscopy. Anal. Rev. Phys. Chem. 2010; 61:263–282.

(24). Lima FA, Milne CJ, Amarasinghe DCV, Rittmann-Frank MH, van der Veen RM, Reinhard M, Pham V-T, Karlsson S, Johnson SL, Grolimund D, Borca C, et al. A High-Repetition Rate Scheme for Synchrotron-Based Picosecond Laser Pump/X-Ray Probe Experiments on Chemical and Biological Systems in Solution. Rev. Sci. Instrum. 2011; 82:063111. [PubMed: 21721678]

(25). March AM, Stickrath A, Doumy G, Kanter EP, Krässig B, Southworth SH, Attenkofer K, Kurtz CA, Chen LX, Young L. Development of High-Repetition-Rate Laser Pump/X-Ray Probe Methodologies for Synchrotron Facilities. Rev. Sci. Instrum. 2011; 82:073110. [PubMed: 21806175]

(26). Bailey JA, Hill MG, Marsh RE, Miskowski VM, Schaefer WP, Gray HB. Electronic Spectroscopy of Chloro(terpyridine)platinum(II). Inorg. Chem. 1995; 34:4591–4599.

(27). Thiel DJ, Livins P, Stern EA, Lewis A. Microsecond-Resolved XAFS of the Triplet Excited State of Pt2(P2O5H2)4. Nature. 1993; 362:40–43. [PubMed: 8383295]

(28). Scheuring EM, Clavin W, Wirt MD, Miller LM, Fischetti RF, Lu Y, Mahoney N, Xie A, Wu J, Chance MR. Time-Resolved X-ray Absorption Spectroscopy of Photoreduced Base-off Cob(II)alamin Compared to the Co(II) Species in Clostridium Thermoaceticum. J. Phys. Chem. 1996; 100:3344–3348.

(29). Wang H, Peng G, Cramer SP. X-ray Absorption Spectroscopy of Biological Photolysis Products: Kilohertz Photolysis and Soft X-Ray Applications. J. Electr. Spec. Rel. Phenomena. 2005; 143:1–7.

(30). Haumann M, Liebisch P, Müller C, Barra M, Grabolle M, Dau H. Photosynthetic O2 Formation Tracked by Time-Resolved X-ray Experiments. Science. 2005; 310:1019–1021. [PubMed: 16284178]

(31). Tovrog BS, Kitko DJ, Drago RS. Nature of the Bound Oxygen in a Series of Cobalt Dioxygen Adducts. J. Am. Chem. Soc. 1976; 98:5144–5153.

(32). Pantani O, Naskar S, Guillot R, Millet P, Anxolabéhère-Mallart E, Aukauloo A. Cobalt Clathrochelate Complexes as Hydrogen-Producing Catalysts. Angew. Chem. Int. Ed. 2008; 47:9948–9950.

(33). Stojanoff V, Hämäläinen K, Siddons DP, Hastings JB, Berman LE, Cramer S, Smith G. A High-resolution X-Ray Fluorescence Spectrometer for Near-Edge Absorption Studies. Rev. Sci. Instrum. 1992; 63:1125–1127.

(34). Kleymenov E, van Bokhoven JA, David C, Glatzel P, Janousch M, Alonso-Mori R, Studer M, Willimann M, Bergamaschi A, Henrich B, et al. Five-Element Johann-Type X-Ray Emission Spectrometer with a Single-Photon-Counting Pixel Detector. Rev. Sci. Instrum. 2011; 82:065107. [PubMed: 21721730]

(35). Glatzel P, Bergmann U. High Resolution 1s Core Hole X-ray Spectroscopy in 3d Transition Metal Complexes—Electronic and Structural Information. Coord. Chem. Rev. 2005; 249:65–95.

(36). Glatzel P, Sikora M, Smolentsev G, Fernández-García M. Hard X-ray Photon-in Photon-out Spectroscopy. Catalysis Today. 2009; 145:294–299.

(37). Vankó G, Bordage A, Glatzel P, Gallo E, Rovezzi M, Gawelda W, Galler A, Bressler C, Doumy G, March AM, et al. Spin-State Studies with XES and RIXS: From Static to Ultrafast. J. Electr. Spec. Rel. Phenomena.

(38). Cammarata M, Eybert L, Ewald F, Reichenbach W, Wulff M, Anfinrud P, Schotte F, Plech A, Kong Q, Lorenc M, et al. Chopper System for Time Resolved Experiments with Synchrotron Radiation. Rev. Sci. Instrum. 2009; 80:015101. [PubMed: 19191457]

(39). Graber T, Anderson S, Brewer H, Chen Y-S, Cho HS, Dashdorj N, Henning RW, Kosheleva I, Macha G, Meron M, et al. BioCARS: a Synchrotron Resource for Time-Resolved X-ray Science. J. Synchrotron Rad. 2011; 18:658–670.

(40). Nozawa S, Adachi S, Takahashi J, Tazaki R, Guérin L, Daimon M, Tomita A, Sato T, Chollet M, Collet E, et al. Developing 100 ps-Resolved X-ray Structural Analysis Capabilities on Beamline NW14A at the Photon Factory Advanced Ring. J. Synchrotron Rad. 2007; 14:313–319.

(41). Haldrup K, Harlang T, Christensen M, Dohn A, van Driel TB, Kjær KS, Harrit N, Vibenholt J, Guerin L, Wulff M, et al. Bond Shortening (1.4 Å) in the Singlet and Triplet Excited States of [Ir2(dimen)4]2+ in Solution Determined by Time-Resolved X-ray Scattering. Inorg. Chem. 2011; 50:9329–9336. [PubMed: 21823573]

(42). Ejdrup T, Lemke HT, Haldrup K, Nielsen TN, Arms DA, Walko DA, Miceli A, Landahl EC, Dufresne EM, Nielsen MM. Picosecond Time-Resolved Laser Pump/X-ray Probe Experiments Using a Gated Single-Photon-Counting Area Detector. J. Synchrotron Rad. 2009; 16:387–390.

(43). Haldrup K, Vankó G, Gawelda W, Galler A, Doumy G, March AM, Kanter EP, Bordage A, Dohn A, van Driel TB, et al. Guest–Host Interactions Investigated by Time-Resolved X-ray Spectroscopies and Scattering at MHz Rates: Solvation Dynamics and Photoinduced Spin Transition in Aqueous Fe(bipy)32+ J. Phys. Chem. A. 2012; 116:9878–9887. [PubMed: 22970732]

(44). Jennings G, Jager WJH, Chen LX. Application of a Multi-Element Ge Detector in Laser Pump/X-Ray Probe Time-Domain X-Ray Absorption Fine Structure. Rev. Sci. Instrum. 2002; 73:362–368.

(45). Stern EA, Heald SM. An X-Ray Filter Assembly for Fluorescence EXAFS Measurements. Nucl. Instrum. Meth. 1980; 172:397–399.

(46). Bewer B. Soller slit design and characteristics. J. Synchrotron Rad. 2012; 19:185–190.

(47). Smolentsev G, Guilera G, Tromp M, Pascarelli S, Soldatov AV. Local Structure of Reaction Intermediates Probed by Time-Resolved X-Ray Absorption Near Edge Structure Spectroscopy. J. Chem. Phys. 2009; 130:174508. [PubMed: 19425791]

(48). Smolentsev G, Canton SE, Lockard JV, Sundstrom V, Chen LX. Local Structure of Photoexcited Bimetallic Complexes Refined by Quantitative XANES Analysis. J. Electr. Spec. Rel. Phenomena. 2011; 184:125–128.

(49). Haldrup K, Christensen M, Cammarata M, Kong Q, Wulff M, Mariager SO, Bechgaard K, Feidenhans'l R, Harrit N, Nielsen MM. Structural Tracking of a Bimolecular Reaction in Solution by Time-Resolved X-Ray Scattering. Angew. Chem. Int. Ed. 2009; 48:4180–4184.

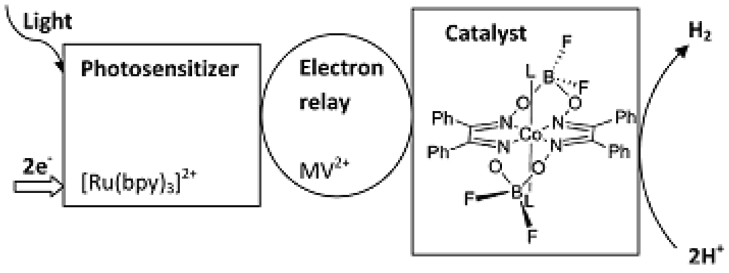

Fig. 1. Scheme of hydrogen evolution by multicomponent photocatalytic system.
The structure of cobaloxime $[Co(dpgBF_2)_2L_2]$ is also shown, with L representing the solvent molecule.

Europe PMC Funders Author Manuscripts

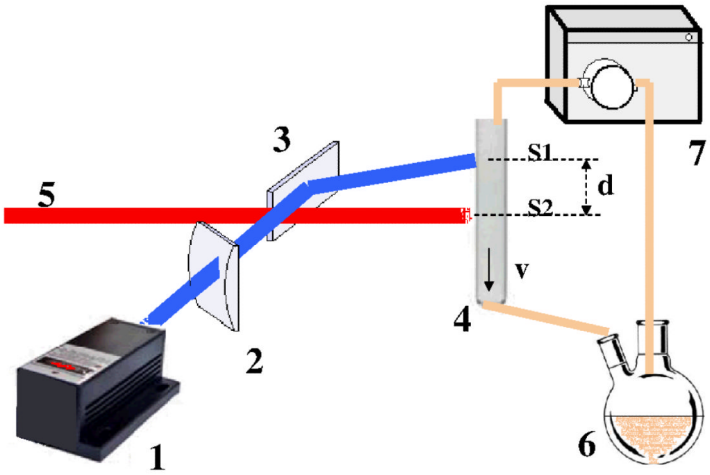

Fig. 2. Scheme of the setup for the pump-flow-probe experiment.

(1) CW laser, (2) cylindrical lenses for focusing, (3) mirror, (4) capillary with continuously flowing sample, (5) X-ray beam, (6) reservoir with the sample, (7) gear pump. The vertical size of the laser beam is **S1** and of the X-ray beam is **S2**. The distance between laser and X-ray beams is d and average flow speed of the sample in the capillary is v.

Europe PMC Funders Author Manuscripts

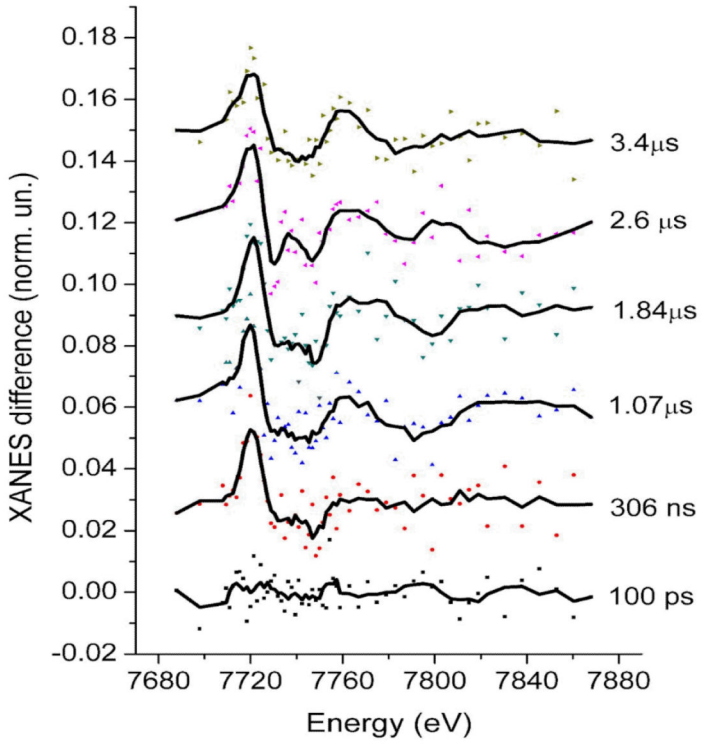

Fig. 3. Co K-edge X-ray transient absorption spectra of the multicomponent Ru/MV/Co photocatalytic system corresponding to a series of different time delays between laser and X-ray pulses and acquired using the pump-sequential-probes method.

Dots correspond to the measured data points while lines are the smoothed spectra (adjacent averaging with window of 5-points). Error bars have been omitted for clarity, but the measurement uncertainty is well-represented by the scatter around the averaged curve.

Europe PMC Funders Author Manuscripts

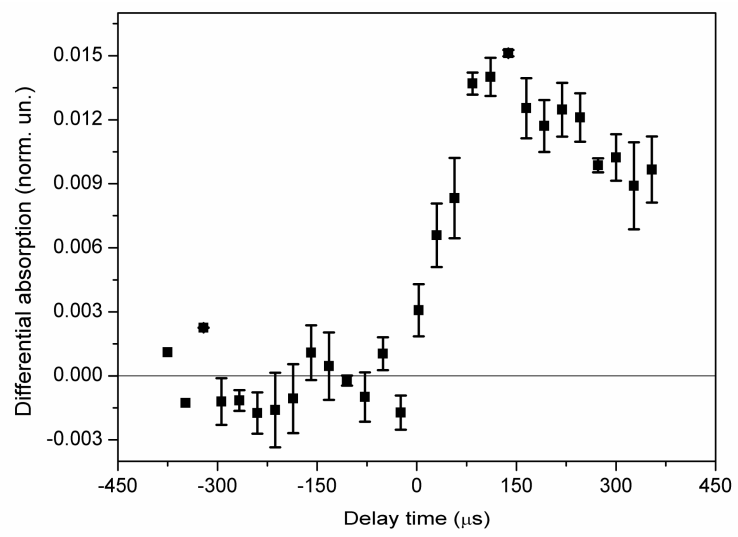

Fig. 4. Transient X-ray absorption signal as a function of delay time between laser and x-ray beams in the pump-flow-probe experiment, measured at the energy of the first maximum of the transient XAS spectrum (7720 eV) associated with Co reduction.

The delay between pump and probe is defined by the relative position of the beams in the pump-flow-probe configuration.

Europe PMC Funders Author Manuscripts

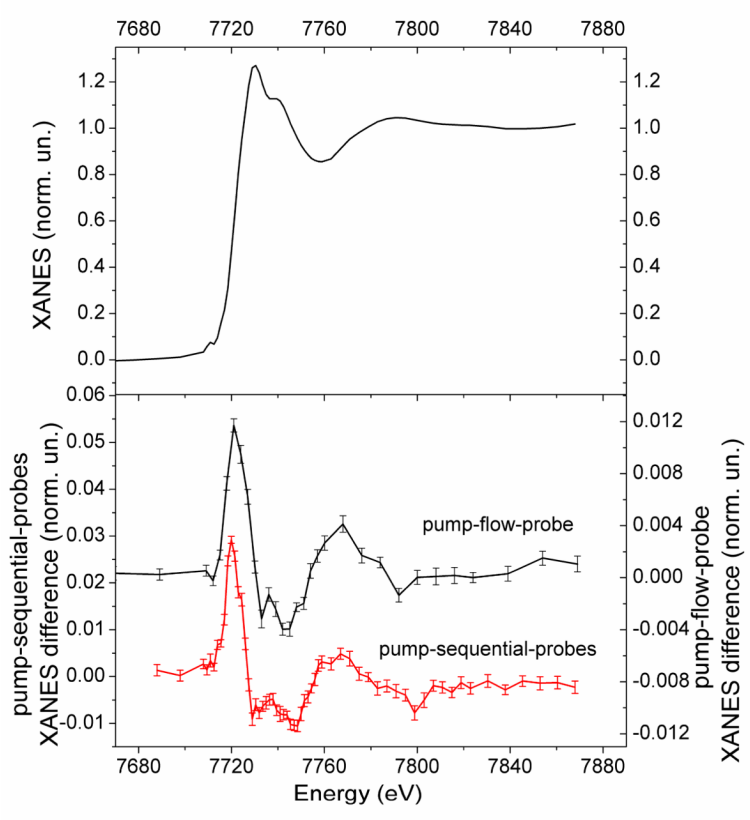

Fig. 5. Top: Co K-edge XANES of the multicomponent Ru/MV/Co photocatalytic system in the ground state. Bottom: Transient X-ray absorption spectra of the Ru/MV/Co measured at the Co K-edge using the pump-flow-probe and pump-sequential-probes methods.

Europe PMC Funders Author Manuscripts

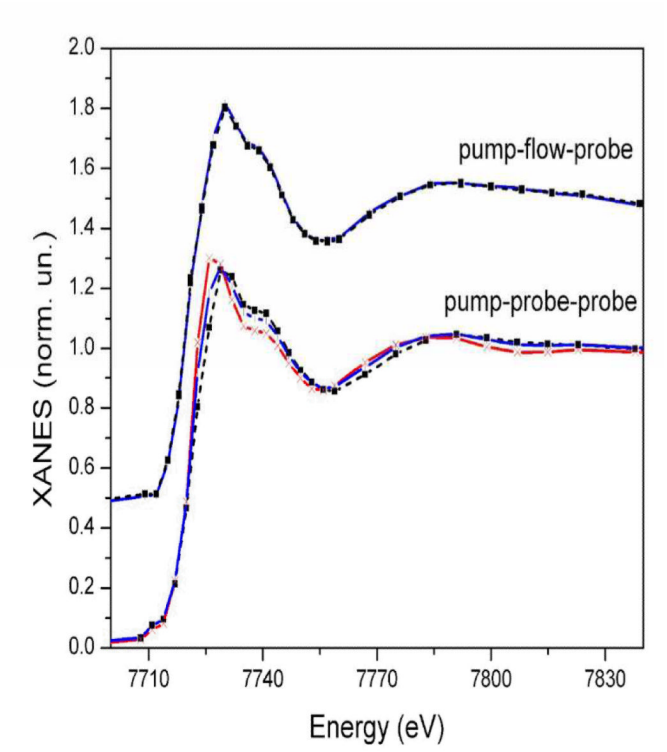

Fig. 6. Effect of sample degradation during measurements using pump-flow-probe (top), and pump-sequential-probes (bottom).

Ground state Co K-edge XANES spectra of the Ru/MV/Co sample before (black dashed lines), after 8 hours (blue lines) and 18 hours (red line) of time-resolved measurements.

Europe PMC Funders Author Manuscripts

Table 1

Statistics of X-ray and laser photons corresponding to the spectra shown in Figs. 3 and 5

	Pump-sequential-probes	**Pump-flow-probe**
Incident flux (ph/s)	$6.5*10^{12}$	$4*10^{11}$
Total number of fluorescent photons/s	$7*10^{9}$	$3*10^{8}$
Total counts/s of the detector	$1.9*10^{7}$	$6*10^{5}$
Total counts/s of the detector for each time point	$2.9*10^{3}$	$6*10^{5}$
Counts/s for selected energy ROI	--	$1.2*10^{5}$
Detected fluorescent counts/s	$2*10^{3}$	$4.8*10^{4}$
N_{eff} Effective number of counts/s	$1.4*10^{3}$	$2*10^{4}$
Parameters of accumulation	4 s/point 40 spectra 60 points	30s/point 20 spectra 30 points
Total dose of laser radiation (photons)	$1.3*10^{22}$	$4*10^{22}$
Total X-ray dose (photons)	$6.2*10^{16}$	$1.4*10^{16}$
Accumulated effective “laser on” X-ray counts/point	$2.2*10^{5}$	$1.2*10^{7}$
Expected Noise of the difference signal normalized to the absorption edge jump	$3.3*10^{-3}$	$5.6*10^{-4}$
Observed noise (Average error above the edge)	$5*10^{-3}$	$5.4*10^{-4}$